

## ***Interactive comment on “The faint young Sun problem revisited with a 3-D climate-carbon model – Part 1” by G. Le Hir et al.***

**G. Le Hir et al.**

lehir@ipgp.fr

Received and published: 17 July 2013

The faint young Sun problem revisited with a 3D climate-carbon model - Part I

Guillaume Le Hir<sup>1</sup>, Yoram Teitler<sup>1</sup>, Frédéric Fluteau<sup>1</sup>, Yannick Donnadieu<sup>2</sup> & Pascal Philippot<sup>1</sup> <sup>1</sup> IPGP, Université Paris 7-Denis Diderot, 1 rue Cuvier, 75005 Paris, France <sup>2</sup> LSCE, CNRS-CEA-UVSQ, 91191 Gif-sur-Yvette, France keywords : faint young Sun, early Earth, climate modelling, Archean, pCO<sub>2</sub>

Considering the weak luminosity of the early Sun, it is generally inferred that high concentrations of greenhouse gases (CO<sub>2</sub>, CH<sub>4</sub>) are required to prevent the early Earth's surface temperature to drop below the freezing point of liquid water. Conversely, a new controversial assumption based on banded iron formation mineralogy hypothesizes

C1494

that the Archean atmosphere was potentially characterized by low concentrations of CO<sub>2</sub>. To solve the faint young Sun problem, it was suggested that a reduced albedo associated to less reflective clouds was able to prevent the Earth to jump into a snowball state. In this very active debate, we have investigated the early Earth climate using a general circulation model to test this scenario. Our simulations include the ice albedo feedback and specific Archean climatic factors such as a high CH<sub>4</sub> concentration, a different cloudiness, a faster Earth's rotation rate and a reduced continental surface. We demonstrate that when larger cloud droplets are accounted for, clouds warm high latitudes and inhibit sea-ice formation. This process limits the ice-albedo feedback efficiency and may prevent a global glaciation. Due to this particular mechanism, low pCO<sub>2</sub> allow maintaining a mild climate during the early Archean. The carbon cycle-climate interplays and conditions sustaining pCO<sub>2</sub> will be discussed in the companion paper.

### 1. Introduction

Sagan and Mullen (1972) argued from solar models that, in the early Archaean, the Sun, as a relatively young star, would have had 25% lower luminosity than it does now. According to climate models, the weakness of the young Sun's brightness would have meant Earth's surface temperature was well below freezing point in the first two billion years. A completely frozen Earth, however, conflicts with evidence of the presence of liquid water at the surface and life development during the Archaean. Greenhouse gases, and more particularly carbon dioxide, were soon put forward as good candidates for solving this problem (see Feulner 2012 for a detailed review, Wordsworth and Pierrehumbert 2013), known as the 'faint young Sun paradox' (hereafter FYSP). Using a vertical one-dimensional radiative convective climate model (hereafter RCM), Kasting (1984) calculated that, for 4Ga solar luminosity (75% of its present-day value), a pCO<sub>2</sub> of 0.3bar or ~1000 times the preindustrial atmospheric level (PAL) (i.e. 0.28 mbar or 280 ppm) was needed to maintain a mean global surface temperature of 288K.

In parallel with the modelling approach, in the mid-nineties carbon dioxide was semi-

C1495

quantitatively estimated from Archaean palaeosols. Because of the absence of siderite in 2.8 Ga old soils, Rye et al (1995) suggested that the  $p\text{CO}_2$  had not exceeded  $\sim 0.03$  bar (or  $\sim 100$  PAL). Their mineralogical approach was questioned by Sheldon (2006). Using a mass-balance approach, Sheldon (2006) suggested that the  $p\text{CO}_2$  was more probably about 8.5 mbars plus or minus a factor of three (i.e.  $24 \times 3/3$  PAL) between 2.2 and 1.0 Ga. Furthermore, in a recent study by Driese and collaborators (2011), palaeoweathering indicators were used to support the assumption of moderate  $\text{CO}_2$  partial pressures, at around 10mbar at 2.7Ga. Rosing et al (2010) further lowered the atmospheric  $\text{CO}_2$  concentration. Given the composition of iron-rich minerals found in Archaean banded iron formations (BIF), they argued that the coexistence of magnetite (i.e.  $\text{Fe}_3\text{O}_4$ , a moderately oxidised mineral) and siderite (i.e.  $\text{FeCO}_3$ , a reduced mineral) in BIF was dependent on the atmospheric level in di-hydrogen ( $\text{pH}_2$ ). Di-hydrogen ( $\text{H}_2$ ) is a nutrient for methanogenic bacteria, and biological constraints impose a minimum  $\text{pH}_2$ . Using this constraint, Rosing et al (2010) defined an upper limit for  $p\text{CO}_2$  close to 0.9 mbar (900 ppmv or 3.2 PAL). Such a low  $p\text{CO}_2$  has been abundantly discussed notably because BIF was probably formed far from the thermodynamic equilibrium with the atmosphere (Dauphas and Kasting 2011; Reinhard and Planavsky 2011). These estimates of  $p\text{CO}_2$  are in conflict with modeling results. Kienert et al (2012), using an EMIC (Earth System Models of Intermediate Complexity), fix to 0.6 bar the carbon dioxide partial pressure to maintain the surface temperature close to its present-day value (288K). In their study, Kienert et al. (2012) need to increase the  $\text{CO}_2$  partial pressure to compensate for the weaker Sun because their model simulates a larger ice albedo feedback, which they associated with the faster Earth rotation rate. This result is opposed to conclusions obtained by Jenkins with GENESIS (Jenkins, 1993), i.e. a larger rotation rate would have induced warmer climate.

Although an enhanced greenhouse effect seems the most likely solution to the FYSP, other mechanisms influencing climate have been explored, such as changes in cloud properties. The mean forcing of clouds results from two opposite effects. Clouds are highly reflective in the spectrum of visible solar radiation (shortwave radiation) and

C1496

highly absorbent in the spectrum of thermal terrestrial radiation (longwave radiation). This leads to two well-known opposite effects: the reflective effect contributing to the planetary albedo and the longwave absorption contributing to the greenhouse effect. These mechanisms are related to the cloud type, the greenhouse effect being stronger than the albedo effect in the case of cirrus clouds, which are quite transparent at visible wavelengths but good absorbers of thermal terrestrial radiation. Recent studies have proposed to solve the FYSP by changing the clouds. Rondanelli and Lindzen (2010) suggested that a cooling of oceanic surfaces would lead to cirrus formation in the tropics, which would warm the early Earth's surface. This mechanism, known as the 'iris hypothesis' remains highly controversial (Hartmann, D. L., and M. L. Michelsen, 2002a, b). If it is true, the 'iris' mechanism should tend to inhibit the glacial/interglacial cycles. The second hypothesis investigates the influence of cloud properties (Goldblatt and Zahnle 2011; Rossow et al. 1982). To compensate for the weaker solar brightness during the Late Archaean, they estimated that clouds must be 3.5 times thicker than today, stratus (highly reflective clouds) must be absent and the Earth must be entirely cloud-covered. These authors conclude that this scenario is very hypothetical because mechanisms able to change cloud properties in such proportions remain to be found. The last scenario invokes cloud condensation nuclei (i.e. CCN) and the potential existence of clouds with a low albedo during the Precambrian period. In present-day atmosphere, abundant CCN permit the formation of small liquid water droplets leading to optically dense and highly reflective clouds because of their direct scattering effect (Charlson et al. 1987). During the Archaean, this could have been very different because of changes of inorganic and organic fluxes; contributors to CCN would reach 10 to 20% of its natural present-day concentration. As a consequence fewer droplets, but of larger size, should form optically thin clouds characterised by a low scattering of shortwave radiation and shorter lifetime (Kump and Pollard 2008; Rosing et al. 2010). Testing this assumption using a RCM, Rosing et al (2010) have shown that a decrease in surface albedo, owing to a considerably smaller continental area and a more transparent atmosphere in terms of shortwave radiation, may have compensated for the

C1497

weak brightness of the Sun during the Archaean. Using a more realistic treatment of clouds, Goldblatt and Zahnle (2011b) have demonstrated that radiative forcing owing to changes in clouds properties have been overestimated in the Rosing et al. study. (2010).

Because RCMs include a detailed radiative scheme, they are well adapted for studying the climatic impact of the Archaean chemical composition of the atmosphere, particularly the abundance of greenhouse gases. Albeit this approach has improved our understanding of the early Earth and can be considered complex enough to yield a first-order climate response for solving the FYSP (Goldblatt and Zahnle 2011b), crucial mechanisms and feedbacks driving the climatic system are not taken into account in these models: dynamics of atmosphere and clouds interplays or omission of clouds in some cases (for details see Goldblatt and Zahnle, 2011b). If RCMs are able to represent the physics of the atmosphere and surface processes, notably the dependence of the Earth's surface albedo on temperature, Rosing et al. (2010) modeling results are obtained with a surface albedo held constant. Its lack may bias the climate response, especially when the Earth tends to cool (see Pierrehumbert et al. 2011 and Pierrehumbert 2010 for details). Without inclusion of the ice albedo feedback in models, the Earth can be artificially maintained unfrozen. For this reason, Kasting (2010) considered that 3-D climate models could help us to understand the early Earth's climate because they capture the ice albedo feedback and atmospheric dynamics.

To go one step further in the understanding of the FYSP, we used a 3-D climate model, FOAM, to investigate the validity of the assumption of low pCO<sub>2</sub>. To answer this question the study was organised as follows. First, a set of experiments was run to simulate the climate from 3.5 Ga to 1 Ga with a timestep of 250 Ma whereas pCO<sub>2</sub> and pCH<sub>4</sub> were kept fixed. The goal of these experiments was not to test the role of the amount of greenhouse gases but rather to investigate the effect of other important forcing factors existing during the Archaean: solar constant, palaeogeography and amount of continental surface, cloud properties, high salinity of oceans and a faster Earth rotation rate.

C1498

We then performed additional sets of simulations to explore the effects of greenhouse gases (CO<sub>2</sub> and CH<sub>4</sub>) using 3.5Ga conditions to better constrain solutions to the faint Young Sun problem.

## 2. Model Description and Simulation Specifications

### 2.1. Model description

Climate simulations were run with the general circulation climate model (GCM) FOAM 1.5. The atmospheric component of FOAM is a parallelised version of NCAR's Community Climate Model 2 (CCM2) with the upgraded radiative and hydrologic physics incorporated in CCM3 v. 3.2 (Jacob 1997). All simulations were performed with an R15 spectral resolution (4.5° × 7.5°) and 18 vertical levels. FOAM is used in mixed-layer mode, meaning the atmospheric model is linked to a 50-meter mixed-layer ocean with heat transport parameterised through diffusion. The sea ice module uses the thermodynamics of NCAR's to compute ice fraction (growth and melting), snow cover, penetrating radiation with brine pockets, and includes a Semtner model to calculate the sea ice temperature. Sea ice albedo is fixed to 0.7 (visible spectrum) and 0.5 (near-infrared spectrum). The sea ice module does not treat sea-ice dynamics, which may tend to decrease the sea ice cover (Voigt and Abbot, 2012) and overestimate the Earth's cooling. The radiative code (extracted from NCAR CCM3) has already shown its validity in atmospheres highly enriched in CO<sub>2</sub> (Pierrehumbert 2004, Le Hir et al., 2010). The infra-red absorption has been computed (figure 1) to replace CO<sub>2</sub>, CH<sub>4</sub> conversion proposed by Rosing et al (2010). Under an enriched CH<sub>4</sub> atmosphere no large differences are observed compared to prior estimates (Kiehl and Dickinson, 1987; Halevy et al. 2009).

FOAM, like other GCMs, relies on a physical basis, which means that mechanisms and feedbacks are explicitly represented. Goldblatt and Zahnle (2011b) challenged the use of GCMs given that sub-grid scale parameterisation of clouds in GCM precludes their use in palaeoclimate modelling. Obviously GCMs still have limitations (Hack 1998,

C1499

Abbot et al. 2012, Stevens and Bony, 2013). However, being fully dynamics models, GCMs represent a powerful tool for improving our understanding of the Earth's climate, notably cloud mechanisms involved in global warming (Abbot et al. 2009) as well as in deep-time climate changes (Pollard and Kump 2008). Because GCMs can capture clouds and other factors changing with time (palaeogeography, rotation rate, . . .), the authors assume that GCMs remain accurate tools for investigating past climates (Donnadieu et al. 2009; Donnadieu et al. 2006; Le Hir et al. 2009; Le Hir et al. 2010; Le Hir et al. 2011; Nardin et al. 2010; Poulsen and Jacob, 2004).

## 2.2. Boundary conditions and experimental design

In order to test how solar constant, palaeogeography, amount of continental surface, cloud properties, high salinity of oceans and a faster Earth rotation rate influenced the climate during the Archaean eon, atmospheric partial pressures of both CO<sub>2</sub> and CH<sub>4</sub> were fixed at 900 ppmv or 0.9 mbar. These greenhouse gases concentrations have been fixed to respect values used by Rosing et al. 2010, a necessary condition to compare both studies. We point that no valid argument, evoked in Rosing et al (2010), supports such low pCO<sub>2</sub> values (Dauphas and Kasting 2011; Reinhard and Planavsky 2011). The high CH<sub>4</sub> value is more realistic (Pavlov et al. 2000), but only before the Great Oxidation Event (2.4Ga) when the atmosphere was anoxic and once methanogens evolved. Unfortunately when a large mixing ratio of methane is considered, an organic haze should be formed (CH<sub>4</sub>/CO<sub>2</sub> > 0.2) (Haqq-Mishra et al. 2008). To resolve the problem of organic haze formation or unrealistic high methane levels after the Great Oxidation Event, the high CH<sub>4</sub> could be brought down by substituting CO<sub>2</sub> (in Figure 1, one can see that 900ppmv of CO<sub>2</sub> and CH<sub>4</sub> correspond to 100 ppmv for CH<sub>4</sub> and 2000 ppmv for CO<sub>2</sub>). Because of the quasi-absence of oxygen in the Archaean atmosphere (Bekker et al. 2004), the stratospheric ozone layer was removed for all experiments prior to 2.25 Ga and remained at present-day value for all experiments of the Proterozoic aeon. The absence of the ozone layer precluded the formation of a stratospheric temperature inversion. It resulted in a 40 km thick atmo-

C1500

sphere without temperature stratification (corresponding to the topmost atmospheric grid points in the GCM). The global mean lapse rate between the surface and the 200 hPa level was not significantly affected by the absence of the ozone layer, and a mean global cooling of 0.7°C only at the Earth surface was simulated (Appendix A). The atmospheric thermal structure resulting from the removal of the ozone layer agreed well with previous studies. A 1-D climate model was used, which estimated cooling in the range of 1 to 2°C at the Earth's surface (Kasting et al. 1984; Kiehl and Dickinson 1987). Orbital parameters were set at their present-day values (orbital eccentricity: 0.016724, obliquity: 23.4463, vernal equinox latitude of perihelion: 77.9610) in all experiments. Finally the diffusion rate of the slab ocean is held constant to its present-day value.

We performed a first set of numerical experiments for the period ranging from 3.5 to 1 Ga with a 0.25 Gyr time step (Table 1a). Boundary conditions including solar constant and palaeogeography changed dramatically in this period of 2.5Gyr. Indeed the solar constant increased by as much as 19% between 3.5 Ga (1053 W/m<sup>2</sup>) and 1 Ga (1258 W/m<sup>2</sup>) (Gough 1981) (Figure 2a). The early Earth's surface varied in response to the growth and emergence of the continental surface, a process which affected the mean surface albedo ( $\alpha_{\text{ocean}} = 0.06$ ,  $\alpha_{\text{bare soil}} = 0.32$ ). Different scenarios ranging from a progressive formation to a quasi-instantaneous formation of all continental crust have been proposed. Here we considered a gradual continental growth (Figure 2b), an evolution in agreement with the changes of 87Sr/86Sr (Godderis and Veizer 2000) and  $\delta^{34}\text{S}$  throughout the Archaean and Early Proterozoic. According to this scenario, the surface of the emerged continents changed from 4% at 3.5 Ga to 27.5% at 1 Ga. The palaeogeography were reconstructed based on paleomagnetic data (Pesonen et al., 2003) which were available for this deep time period (Figure 2c). 3.5 to 2.75Ga reconstructions are theoretical, the continents were assumed located at low and mid latitudes. The elevation of land points was fixed at 200 m in all experiments.

In order to test the impact of modern clouds on the Earth's energy budget, a set of experiments has been also performed in which clouds were totally removed (Table 1a).

C1501

To quantify how larger liquid droplets influence climate, we performed an additional set of experiments in which the mean diameter radius of liquid droplets was modified as suggested by Rosing et al (2010) (i.e. fixed at  $20\ \mu\text{m}$  over oceans and continents, see Table 1a). Larger liquid water droplets ( $20\ \mu\text{m}$ ), about twice the mean present-day size (5 to  $10\ \mu\text{m}$  over continents, and  $10\ \mu\text{m}$  over oceans), are the direct result from lower atmospheric concentration in CCN. Reasons supporting the low CCN hypothesis throughout the Archean remain hypothetical but not unrealistic. Based on considerable progress in understanding main factors enable to act as CCN (Andrea and Rosenfeld, 2008 and citations therein), we could suspect that in absence of dimethylsulphide (or DMS) produced by planktonic eukaryotic algae (Charlson et al. 1987, and citations therein) biological sources of CCN should be reduced. For inorganic sources, the absence of important emerged terrestrial surfaces, source of soil dust, dramatically reduces CCN emissions. Supposing that sea salt (1st source of CCN) contributes only a small fraction of the cloud active particles due to their very coarse size, and that volcanism was mainly submarine (sulphate aerosols contributor), the CCN availability would be lowered relative to present day. These geological assumptions underlie that the early Archean would be characterized by fewer CCN's and large droplets clouds. These larger droplets rain out more rapidly increased cloud-to-precipitation conversion rates. To take this factor into account which was omitted in Rosing and collaborators' study (2010), we used the dependency established by Kump and Pollard (2008), fixing this ratio at eight (instead of one for current conditions). Literature presents a wide range of possibilities for the parameterization of enhanced rain-out (Goldblatt and Zahnle, 2011b, Penner et al. 2006). Here, we used this dependency as reference because it is an intermediate value, which suggests a mid-strength feedback. In absence of a cloud microphysics module, only droplet radii are changed, with no prescribed change to cloud lifetime.

To complete this work, we conducted an additional set of experiments in order to determine whether a faster Earth rotation rate, a saltier ocean or both would affect the previous results keeping held constant other boundary conditions (summarize avail-

C1502

able table 1b). Indeed Palaeozoic rhythmites, mollusc shells and coral fossil records indicate that the Earth rotated faster in the deep past leading to a shorter length of the day (LOD) (Walker and Zahnle 1986). Between 3.8 and 2.5 Ga, the slowdown of the rotation rate increased the LOD from 14 to 18 hours. Jenkins (1993) and Jenkins et al (1993) tested the effects of a shorter LOD on the early Earth climate using a GCM. He demonstrated that a faster rotation (corresponding to an LOD of  $\sim 14$  hours) reduces the mean global cloudiness by 20% and increases the mean global surface temperature by  $2^\circ\text{C}$ . In fact global warming hides local temperature changes, namely a cooling at the poles and a warming in the tropics because of the weakening of transient eddies carrying the heat from low to high latitudes. Hence faster Earth rotation may render the Earth more vulnerable to the ice albedo feedback (Kienert et al. 2012). To check this assumption, we ran a set of experiments for an LOD of 16 hours which corresponded to an LOD 3.5 Ga ago. Another peculiar feature of the Archaean Earth is the hypersaline ocean. Hay and collaborators (2006) revealed large-scale salinity changes over the course of the Phanerozoic, owed to fluctuations in the total salt content of oceans. Knauth (2005) suggested a long-term decline of ocean salinity throughout the Precambrian in parallel with the development of sedimentary basins and climatic conditions able to form and preserve halite (NaCl) deposits. In consequence the Archaean oceans could have been rich in  $\text{Na}^+$  leading to a mean salinity close to 60% at that time (in comparison with 35% at the present day) (Knauth 2005; Foriel et al. 2009). Because a higher salinity lowers the seawater freezing temperature (Millero and Poisson, 1981), sea ice formation could have been delayed and potentially limited the influence of ice albedo feedback. Because the GCM FOAM is coupled with a slab ocean, a higher salinity cannot be taken into account. To mimic this feature, we fixed the seawater freezing point at  $-3.3^\circ\text{C}$  following the equation of state of seawater proposed by Millero and Poisson (1981). As regards the LOD experiments, the influence of hypersaline ocean was only tested for 3.5Ga, which represents the most severe conditions for solving the FYSP.

### 3. Influence of Archaean Factors

C1503

Figure 3 shows the global mean surface temperature (3a) and the mean planetary albedo (3b). To avoid any effect of initial conditions, for each time slice, simulations started from warm initial conditions (present-day as starting point) and go toward colder conditions (Sun brightness decreasing). Each run lasts several tens of years until a steady state is reached for a decade or more. Climatic variables are averaged over the last decade. All simulations are summarized in table 1a.

### 3.1. Influence of the solar constant

Figure 3a (blue curve) represents the global mean surface temperature (i.e.  $T_s$ ) from 3.5 Ga to 1 Ga simulated by using the present-day cloud parameterisation. The mean temperature is as low as  $-75^\circ\text{C}$  at 3.5 Ga and increases linearly up to  $-65^\circ\text{C}$  at 2.5 Ga. The planetary albedo always exceeds 0.65 (Figure 3b, blue curve) because the Earth is entirely frozen. An abrupt climatic bifurcation expressed by temperature and albedo shifts is observed between the 2.5 Ga and 2.25 Ga experiments. The global mean surface temperature reaches  $-20^\circ\text{C}$  in the 2.25 Ga run and the albedo falls to 0.45. It corresponds to a partially frozen Earth; sea ice spreads up to  $30^\circ$  latitude in both hemispheres. Between 2.25 Ga and 1.75 Ga, we observe a slight global warming of about  $5^\circ\text{C}$  followed by a marked change of some  $24^\circ\text{C}$  between 1.75 Ga and 1.25 Ga and a final slight warming of  $4^\circ\text{C}$  between the two last runs at 1.25 and 1 Ga, respectively.

Three climate states can be defined: a weakly frozen Earth (1 Ga and 1.25 Ga), a partially frozen Earth (from 1.75 Ga to 2.25 Ga) and a snowball Earth (2.5 Ga and beyond). We note that the changes in global mean surface temperature during this interval are far from linear (Figure 3a), albeit the solar brightness increases almost linearly. The solar brightness at 1 Ga and 1.25 Ga is strong enough to limit the sea ice extent at the latitude of  $50$  to  $60^\circ$ . The mean latitudinal surface temperature gradient does not significantly differ from the present-day one. Between 1.25 Ga and 1.75 Ga, sea ice spreads towards the equator up to  $30^\circ\text{C}$  in response to the decrease in solar incoming radiation. Between 1.75 Ga and 2.25 Ga, the sea ice limit remains fixed in the

C1504

vicinity of  $30^\circ\text{C}$ . Indeed sea ice cannot stretch further towards the equator because of the strong meridional energy transport by atmosphere and ocean driven by a latitudinal gradient of temperature about twice as strong as in the 1Ga experiment. Finally, as the solar brightness still decreases, we jump into a climate state corresponding to an entirely frozen Earth. Hence, for fixed greenhouse-gas concentrations, the solar constant evolution and its interplay with the ice albedo feedback are the predominant factor governing the Earth's climate. The use of a 3D model (GCM) highlights the nonlinear compartment of the climate, notably a jump into a snowball state; results are at odds with the recent work of Rosing et al. (2010) with a 1D model (RCM) where abrupt climatic bifurcations are not observed because of the absence of ice-albedo feedback

### 3.2. Influence of clouds

To highlight the prevailing role of clouds, new experiments were performed without the formation of clouds (no-clouds runs, see green lines on Figure 3). The set of experiments yields two climatic states. The first state corresponds to a snowball Earth (from 3.5 to 2.5 Ga), where the global mean surface temperature is very similar to those simulated with modern clouds. The bifurcation from a snowball state toward a partially ice-free Earth takes place at the same time (between 2.5 Ga and 2.25 Ga). This apparent similarity in the snowball Earth bifurcation is an artifact. The 0.25 Gyr time step is too crude to distinguish these two cases. A 0.25 Gyr time step induces a significant change in term of incoming energy received, here estimated to  $\Delta F = -6\text{W/m}^2$  (Figure 2). Tropical surface temperatures of the no-clouds run at 2.25Ga (green square, Figure 3a) being just  $5^\circ\text{C}$  warmer than clouds run's temperature (blue square, Figure 3a), the negative forcing provided by the solar brightness decrease contributed to extend the sea ice and generate a cooling in tropics. This irreversible tendency might be amplified by the clouds scheme of FOAM that tends to underestimate the cloud radiative forcing (CRF) in a cold climate (Abbot et al. 2012).

We observe, however, that when clouds are removed, the global mean surface tem-

C1505

perature at 2.25 Ga is 15°C warmer and increases quasi-linearly to reach 20°C at 1 Ga. This result agrees with the CRF, predicting a negative forcing from -10 to -20 W/m<sup>2</sup> at high and mid-latitudes when modern cloud parameterization is used (Figure 4b). In consequence the removal of clouds limits sea ice migration beyond the mid-latitudes. This result explains the slowdown of global warming after 1.5 Ga obtained with no-clouds runs (Figure 3a, green curve) because sea ice is restricted at very high latitudes and its contribution to planetary albedo becomes insignificant (Figure 3b, green curve). This mechanism, and the absence of clouds in the planetary albedo (p-albedo) computation, explains why no-clouds experiments present the lowest p-albedo after 2.5 Ga (Figure 3b, green curve). These simulations also show that modern clouds, with their negative CRF in mid-high latitudes, enhance the Earth's climate sensitivity to ice albedo feedback, which tends to amplify the Earth's cooling.

Finally we investigated the role of low CCN clouds (Figure 3, red curves). The use of large liquid droplets (20 μm) promotes a climatic bifurcation at 3 Ga some 0.75 Gyr earlier compared with the other sets of experiments. Snowball Earth states characterised by a global mean surface temperature of -70°C are simulated at 3.5 Ga and 3.25 Ga only, when the incoming solar energy is too weak to prevent Earth's surface from complete freezing. In the 3 Ga experiment, the global mean surface temperature is about 13°C and then increases linearly approaching 31°C in the last experiment at 1 Ga. Throughout the Archaean and Proterozoic aeons, low CCN clouds increase the global mean surface temperature by 20°C to 35°C, at 1 Ga and 2.25 Ga respectively. Moreover, just before the snowball state bifurcation, the predicted climate is temperate, 13°C in terms of global annual mean (Figure 3a, red curve), differently from other situations (-5° and -20°C for modern clouds and no-cloud runs respectively, see Figure 3a blue and green curves). These very warm temperatures and the bifurcation from an ice-free Earth to a snowball Earth at 3 Ga could appear surprising. For that reason, we examined how low CCN clouds affect sea ice formation and its spread to understand this very unusual climate behaviour. The cloud radiative forcing (Figure 4a) shows that net CRF obtained with large droplets (CCN fixed at 20 μm) was positive in all experi-

C1506

ments except during snowball state (Figure 4a). For the 1Ga case, increasing droplets size by 2 gives a net CRF of 14W/m<sup>2</sup> instead of -4W/m<sup>2</sup>, the net forcing is then 18W/m<sup>2</sup> higher, not so far of value found estimated by Goldblatt and Zahnle (2011b). More importantly, with large liquid droplets the CRF is positive at high latitudes (+40 W/m<sup>2</sup>), favouring warming and preventing sea ice formation (Figure 4b), which is the opposite of results obtained using the normal droplet size of clouds (CCN ranging from 5 to 10 μm) (Figure 4a, b). This positive CRF, predicted with low CCN clouds, results from the combination of a slightly more negative CRF at short wavelength (scattering effect) and a much more positive CRF at large wavelength (IR trapping) than with normal size droplets (Figure 4c). As a consequence, even low elevation clouds (the most reflective clouds) have a positive CRF, as already shown by Goldblatt and Zahnle (2011b). Because they inhibit sea ice formation, low CCN clouds limit the ice albedo feedback efficiency, which explains why the p-albedo does not change significantly (Figure 3b, red curve). This process, associated with warming owed to low CCN clouds (Figure 4a), explains the relatively hot surface temperatures obtained from 1 to 3 Ga. This mechanism also allows us to see why the bifurcation from an ice-free Earth to a snowball Earth at 3 Ga is so abrupt. Before 3 Ga the incoming solar energy is too weak and the Earth's cooling reduces the amount of water vapour in the troposphere, which inhibits the condensation of large amounts of water vapour to form low CCN clouds. In these conditions, the ice albedo feedback overcomes effects provided by low CCN clouds, leading to the climatic bifurcation at 3.25 Ga (Figure 3a).

### 3.3 Influence of continental surfaces

The mean albedo of the early Earth's surface has changed in response to the growth of the continental surface ( $\alpha_{\text{ocean}} = 0.06$ ,  $\alpha_{\text{bare soil}} = 0.32$ ). The lower albedo because of the smaller continental area has been suggested as a solution to FYSP (Schatten and Endel 1982; Rosing et al. 2010) and several times dismissed (Walker et al. 1982; Goldblatt and Zahnle 2011). Simulations performed without clouds (Figure 3b, green curve) show that the p-albedo (here equal to surface albedo) was higher at 2.25 Ga

C1507

than at 1 Ga, the opposite of the growth of continents. This p-albedo evolution is caused by the increase of ice coverage associated with the Earth's surface cooling (Figure 3a, green curve). Indeed, a little change in ice surface ( $\alpha_{\text{sea-ice}} = 0.5$ ) is enough to overcome the influence of smaller continental area ( $\alpha_{\text{sea-ice}} = 0.32$ ). These results demonstrate that the surface albedo is, in the first order, governed by the ice extension; the continental growth is a superimposed factor of second-order importance. This result was confirmed with low CCN cloud simulations, which predicted a quite stable p-albedo from 3 to 1 Ga (Figure 3b, red curve), and the ice albedo feedback is almost shut down (Figure 3c, 1 Ga and 3 Ga cases). Hence smaller continental surfaces do not appear to be a mechanism which can solve the FYSP. We discuss in the second part (see companion paper) how this conclusion can be challenged when the carbon cycle is considered (Walker et al. 1981, Godderis and Veizer, 2000).

#### 3.4. Solutions to the FYSP with high CH<sub>4</sub> and low CCN clouds

Since none of the experiments can entirely solve the FYSP when a pCO<sub>2</sub> of 0.9 mbar (or 900 ppmv or 3.2 PAL) is applied, we investigated the minimal amount of CO<sub>2</sub> required to balance the solar weakness 3.5 Ga ago by performing a second set of simulations using a 900ppmv of CH<sub>4</sub> (table 1b). Progressively increasing the pCO<sub>2</sub>, Figure 5a shows that a pCO<sub>2</sub> of 1.8 mbar (or 1800 ppmv or 6.4PAL) is high enough to avoid a pan-glaciation at 3.5 Ga when low CCN clouds are considered. Solving the FYSP with 1.8 mbar of CO<sub>2</sub> at 3.5 Ga may appear surprising, but the radiative forcing separating a snowball Earth state (3.5 Ga, Figure 3c) and a partially ice-free Earth (3 Ga, Figure 3c) does not exceed 9 W/m<sup>2</sup> (Figure 2a). The radiative forcing owed to the doubling of CO<sub>2</sub> (+4 W/m<sup>2</sup>) associated with the ice albedo feedback can easily compensate for the missing 9 W/m<sup>2</sup>. In consequence, when the atmosphere is poorly enriched with CO<sub>2</sub>, low CCN clouds can protect the Earth from global glaciation during the early Archaean. The realisation that low CCN clouds associated with low pCO<sub>2</sub> can solve the FYSP could be an interesting way to reconcile geochemical and modelling estimates without invoking additional warming mechanisms, including pressure broadening of CO<sub>2</sub> and

C1508

H<sub>2</sub>O by high atmospheric pressure (Goldbatt et al. 2009) or high concentrations of H<sub>2</sub> (Wordsworth and Pierrehumbert 2013). This result also implies that the assumption defended by Rosing and collaborators (2010), i.e. that low pCO<sub>2</sub> is compatible with a solved FYSP, appears theoretically possible. It is important to bear in mind, however, that the pCO<sub>2</sub> threshold value, here 1.8 mbars, can be model-dependent. Indeed the carbon dioxide value could differ according to the model used because of their respective parameterisations.

#### 3.5. Influence of faster Earth rotation rate and saltier oceans

To investigate the sensitivity of the pCO<sub>2</sub> as a function of factors able to warm the early Earth (900 ppmv of pCH<sub>4</sub> and low CCN clouds), an additional set of simulations was performed using: (1) an Earth's rotation rate corresponding to the early Archaean (LOD of 16 hours, Zahnle and Walker 1987) and/or (2) an ocean twice as salty (Knauth 2005; Foriel et al. 2009) (see table 1b). With these new constraints of 3.5 Ga boundary conditions and 900ppmv of CO<sub>2</sub>, all simulations predicted a snowball Earth state (Figure 5a), which means that none of these factors represent a serious solution to the FYSP. A similarly puzzling result was obtained with 1800 ppmv of CO<sub>2</sub>, when Earth was not entirely frozen. Runs depicted in Figure 5a reveal that when faster Earth rotation and saltier ocean are associated, simulations predict a very modest warming (+0.2°C). It is quite surprising because a faster Earth rotation rate and a lower seawater freezing point tend to warm the Earth's surface by several degrees in present-day conditions. The explanation of this unusual scenario is found in the complex interplay between these factors. Regarding SST anomalies (Figure 5b), we observe that the warming associated with a saltier ocean is localised in high latitudes. Delaying sea ice formation, elevated salinity decreases the Earth's sensitivity to the ice albedo feedback, a mechanism very effective in cold climates. More intriguing is the response induced by a faster Earth's rotation rate. In present-day conditions, the change of day length from 24 h to 16 h warms the Earth's surface by about 2°C (from 14.5 to 16.3°C, see Figure in Appendix A), in agreement with previous results (Jenkins 1993). Seen in

C1509

detail, however, this warming is inhomogeneous. Thanks to reduced latitudinal heat transport and changed cloud pattern, a faster Earth rotation warms low latitudes but cools high latitudes (see Figure in Appendix A). In present-day conditions, the cooling of high latitudes and the associated sea ice extent remain limited. On the global scale the warming in low latitudes overcomes the cooling in high latitudes. The behaviour is different during the early Archaean because the climate was slightly colder and no emerged land limited the sea ice spread. Indeed simulations show that shorter LOD has the opposite effect (Figure 5b): the sea ice formation at high and mid-latitudes is eased, increasing the albedo and amplifying the cooling. Hence a shorter LOD in these particular conditions does not increase SST on the global scale. For all these reasons, when shorter LOD and saltier oceans are associated they balance each other (shorter LOD increases the Earth's sensitivity to the ice albedo feedback whereas saltier oceans reduce this sensitivity), which explains why they do not affect the results of the FYSP (Figure 5b).

If the effect of the faster Earth rotation rate appears weak compared with results presented in Kienert and collaborators (2012), it is important to note that their simulations were performed by means of a present-day cloudiness parameterisation. Since the modern nebulosity tends to amplify the Earth's cooling (see Section 3.2), CLIMBER simulations (Kienert et al. 2012) overestimate the ice albedo feedback, which may explain a part of the disagreement between these two studies as to whether pCO<sub>2</sub> can solve the FYSP.

#### 4. Discussion

In order to better represent the dynamics (transport processes) and clouds behavior, we have used a GCM. Accounting for a 25% weaker Sun, we show that several millibars of carbon dioxide seems sufficient to keep the Earth's surface temperature close to its present day value. However several processes are missing in this study. One of them is the absence of chemical reactions within the atmosphere. With a CO<sub>2</sub> minimal value close to 2 mbars and CH<sub>4</sub>/CO<sub>2</sub> ratio reaching 0.5, an organic haze should be

C1510

formed (threshold fixed to 0.2 according to Haqq-Mishra et al. 2008). To avoid haze formation, and according to respective radiative forcing of CO<sub>2</sub> and CH<sub>4</sub>, the atmospheric composition of 2mbars of CO<sub>2</sub> and 900ppmv of methane can be substituted by 4mbars of carbon dioxide and 100ppmv of CH<sub>4</sub> (the minimum value for anoxic atmosphere). A second source of uncertainties is the use of a slab-ocean. With heat transport parameterised through diffusion, the GCM cannot intensify the meridional ocean heat transport toward to smaller land fraction (Endal and Schatten 1982). We also acknowledge that oceans with salinity twice as high should lead to a weaker overturning (Williams et al. 2010). These conflicting assessments concerning ocean circulation, and their respective influence on the FYSP, could be explored using a fully-coupled dynamic ocean model, an investigation which has not been done in this study because of time limitations. The last caveat due to the use of a slab-ocean is the absence of sea ice dynamics which may tend to overestimate the Earth's cooling (Voigt and Abbot, 2012) and increase the pCO<sub>2</sub> required to solve the FYSP.

In addition of uncertainties listed before, our conclusions also largely depend on the boundary conditions we used. Indeed high CH<sub>4</sub> concentration and low C<sub>CN</sub> clouds have largely contributed to lower the carbon dioxide atmospheric level. To determine their effects a last set of simulations has been performed where we fixed methane concentration and mean size of liquid droplets to their present-day values (1.7ppmv and 5-10 $\mu$ m respectively). Details of simulations and global mean surface temperature are given in Table 2. We find that, when methane concentration is fixed at its modern value, a global mean surface temperature close the present-day one is reached for 16 mbars of carbon dioxide (run2, Table 2). This pCO<sub>2</sub> counteracts the negative radiative forcing provided by the drop in pCH<sub>4</sub> ( $\Delta F_{CH_4} = -15W/m^2$ , figure 1), and clearly shows the dependency of our conclusions to methane levels. Using modern clouds, a pCO<sub>2</sub> three times higher (run5, Table 2) would be required to solve the FYSP.

If no other warming process is present, FOAM predicts a minimum of  $\sim 0.016$ bar of CO<sub>2</sub> for a mean temperature  $\sim 15^\circ C$ , a result one order of magnitude below 1D model

C1511

values: 0.2-0.3 at 3.5Ga (Kasting et al. 1984, Von Paris et al. 2008), a result that agrees with geochemical estimates (Rye et al. 1995). This conclusion is also in line with an early atmosphere combining CO<sub>2</sub> and CH<sub>4</sub>. Kiehl and Dickinson (1987) find a mean annual surface temperature of 288 K when a CH<sub>4</sub> mixing ratio of 1000 ppmv was combined with a CO<sub>2</sub> partial pressure of  $\sim$ 0.1 bar. Since the radiative transfer cannot be invoked as an explanation (Figure 1), these changes have to be found elsewhere. Several climatic features are difficult to estimate in 1D model: clouds, vertical lapse rate, heat transport and ice/snow cover. As well demonstrated in Goldbatt and Zahnle (2011b), clouds parameterization in RCM may overestimate the real pCO<sub>2</sub> forcing. Thus clouds scheme is not a way to explain why early Earth's climates predicted with our GCM seem to be warmer than 1D model. Unfortunately we cannot bring a definitive answer; we can only suspect the lapse rate feedback. As shown by Pierrehumbert (2004), lapse rate is governed by a complex interplay of dynamics and convection, and is crucial to drive the greenhouse effect efficiency. This process can be associated to horizontal heat transport by atmospheric motions. Because this process may limit the spreading of sea-ice, it may induce warmer early Earth's climate.

## 5. Conclusion

The fact that all pCO<sub>2</sub> estimated from proxies are clearly below modeling results by one order of magnitude implies that other mechanisms have to be researched to solve the FYSP. Prior works have suggested that other greenhouse gases or pressure broadening or some other effects may have contributed to climatic warming. Based on the idea suggested by Rosing et al (2010), we investigated the influence of CCN on clouds properties and their influence on Earth's climate. In contrast to recent modelling studies defending the ability of high pCO<sub>2</sub> to solve the FYSP, our study explains the mechanisms and feedbacks allowing the existence of a temperate climate since 3.5 Ga with low pCO<sub>2</sub>. We argue that, in an atmosphere poorly enriched with cloud condensation nuclei (CCN), carbon dioxide pressures in the order of magnitude of around several mbars combined to high pCH<sub>4</sub> partial pressure, are able to keep the Earth unfrozen.

C1512

Below this CO<sub>2</sub> threshold, not enough water vapour is maintained in the atmosphere to allow cloud formation, which drives the Earth into a snowball state. Above this threshold, clouds formed by large liquid droplets warm high latitudes and inhibit sea ice formation. This process limits the efficiency of the ice albedo feedback and maintains the Earth's albedo at low values, which prevents the complete freezing of the Earth even with low pCO<sub>2</sub>. This complex interplay between clouds and albedo illustrates the value of GCMs in investigating deep-time climates. If this study improves our understanding of the physical processes which can solve the FYSP in terms of climate, we assume that these results are not a final answer, notably because the assumption of large cloud droplets remains a hypothetical assumption. In order to obtain a complete picture of the FYSP, the next step is to test what levels of CO<sub>2</sub> are possible from a climate-carbon cycle perspective, the atmospheric pCO<sub>2</sub> being governed by the carbon cycle at long-term scale (>1Myr).

Appendix A: (a) temperature gradient as a function of Earth rotation rates. (b) Atmospheric lapse rate of function of ozone layer presence/removal. Simulations performed under present-day boundary conditions (see figure in attachment).

Figures captions

Figure 1 Net long-wave fluxes computed for CO<sub>2</sub> and CH<sub>4</sub> with the FOAM radiative code (NCAR ccm3) (the total atmospheric is held constant, 1bar)

Figure 2: boundary conditions for solar constant (upper part) and continental growth (lower part).  $\eta_{land}$  is the emerged surface/Earth surface ratio (present-day surface is 146.106km<sup>2</sup> or 29% of the Earth surface). Each red square represents boundary conditions used in our sets of simulations.

Figure 3: 3D climate simulations from 3.5 to 1 Gyr. a) Evolution of surface temperature versus time assuming increasing irradiance, linear continental growth and pCO<sub>2</sub> and pCH<sub>4</sub> of 900ppmv. Grey line is from Rosing et al (2010). Blue and red lines were obtained using liquid droplets size of 5 to 10 $\mu$ m (modern clouds) and 20 $\mu$ m (optically

C1513

thinner and short-lived clouds), respectively. Green squares represent the no-clouds scenario. b) Evolution of planetary albedo versus time ( $\alpha_{\text{ocean}}$  0.06,  $\alpha_{\text{rocky desert}}$  0.32,  $\alpha_{\text{seaice}}$  0.5,  $\alpha_{\text{snow}}$  0.8). c) Red stars represent sea-ice extend (white) predicted with runs performed with liquid droplets size of  $20\mu\text{m}$  (fig2a, and b show corresponding temperature/albedo for each simulation).

Figure 4: a) Net cloud radiative forcing (CRF, unit  $\text{W/m}^2$ ) versus time. Blue squares represent runs with modern clouds. Optically thinner clouds (red squares) result in a positive forcing because the effect of infra-red trapping overcomes that of scattering. b) CRF as a function of latitude for simulations performed at 1Ga. The black line represents low CCN clouds (liquid droplets size of  $20\mu\text{m}$ ), dashed line the modern clouds parameterization (liquid droplets size of 5 to  $10\mu\text{m}$ ). c) Simulations performed using 1Ga boundary conditions. Dashed lines represent long-wave (LW) budget of clouds (greenhouse effect), continuous lines their short wave budget (albedo effect).

Figure 5: a) faster rotation rate (16 hours of LOD), saltier ocean and pCO<sub>2</sub> impacts on the FYSP 3.5Ga ago. Red diamonds represent simulations with standard conditions (pCH<sub>4</sub> fixed at 900ppmv, low CCN clouds), yellow diamond (standard cond. + saltier ocean), green diamond (standard cond. + 16h of LOD), blue diamond (standard cond. + saltier ocean + 16h of LOD). At 1800 ppmv of CO<sub>2</sub> the surface temperature reaches 14.2°C, 15.0°C, 14.2°C, 14.4°C, respectively. b) The sea surface temperature (SST) response to a faster rotation rate (LOD) and saltier ocean at a fixed pCO<sub>2</sub> (1.8mbar or 1800ppmv or 6.4 PAL).

#### References:

Abbot, D. S., Huber, M., Bousquet, G., and Walker, C. C.: High-CO<sub>2</sub> cloud radiative forcing feed-back over both land and ocean in a global climate model, *Geophys. Res. Lett.*, 36, L05702, 20 doi:10.1029/2008GL036703, 2009.

Abbot, D. S., Voigt, A., Branson, M., Pierrehumbert, R. T., Pollard, D., Le Hir, G., and Koll, D. D. B.: Clouds and snowball Earth deglaciation, *Geophys. Res. Lett.*, 39,

C1514

L20711,doi:10.1029/2012GL052861, 2012.

Andreae M.O., and Rosenfeld D., Aerosol–cloud–precipitation interactions. Part 1. The nature and sources of cloud-active aerosols, *Earth-Science Reviews* vol89, pp13–41, doi:10.1016/j.earscirev.2008.03.001. 2008,

Bekker, A., Holland, H. D., Wang, P. L., Rumble, D., Stein, H. J., Hannah, J. L., Coetzee, L. L., and Beukes, N. J.: Dating the rise of atmospheric oxygen, *Nature*, 427, 117–120, 2004. 5

Charlson, R. J., Lovelock, J. E., Andreae, M. O., and Warren, S. G.: Oceanic Phytoplankton, atmospheric sulfur, cloud albedo and climate, *Nature*, 326, 655–661, 1987.

Dauphas, N. and Kasting, J. F.: Low p(CO<sub>2</sub>) in the pore water, not in the Archean air, *Nature*, 474, E2–E3, doi:10.1038/nature09960, 2011.

Donnadieu, Y., Godderis, Y., Pierrehumbert, R., Dromart, G., Fluteau, F., and Jacob, R.: 10 A GEOCLIM simulation of climatic and biogeochemical consequences of Pangea breakup, *Geochem. Geophys. Geosys.*, 7, 1–21, doi:10.1029/2006GC001278, 2006.

Donnadieu, Y., Godd' eris, Y., and Bouttes, N.: Exploring the climatic impact of the continental vegetation on the Mesozoic atmospheric CO<sub>2</sub> and climate history, *Clim. Past*, 5, 85–96, doi:10.5194/cp-5-85-2009, 2009. 15

Driese, S. G., Jirsa, M. A., Ren, M., Brantley, S. L., Sheldon, N. D., Parker, D., and Schmitz M.: Neoproterozoic paleoweathering of tonalite and metabasalt: implications for reconstructions of 2.69 Ga early terrestrial ecosystems and paleoatmospheric chemistry, *Precambrian Res.*, 187, 1–17, doi:10.1016/j.precamres.2011.04.003, 2011.

Fulner, G.: The faint young sun problem, *Rev. Geophys.*, 50, RG2006, 20 doi:10.1029/2011RG000375, 2012.

Foriel, J., Philippot, P., Rey, P., Somogyi, A., Banks, D., and Menez, B.: Biological

C1515

control of Cl/Br and low sulfate concentration in a 3.5-Gyr-old seawater from North Pole, Western Australia, *Earth Planet. Sci. Lett.*, 228, 451–463, 2004.

Godderis, Y. and Veizer, J.: Tectonic control of chemical and isotopic composition of ancient oceans: the impact of continental growth, *Am. J. Sci.*, 300, 434–461, 2000.

Goldblatt, C. and Zahnle K. J., Faint Young Sun Paradox remains, *Nature*, 474, E1, doi:10.1038/nature09961, 2011

Goldblatt, C. and Zahnle, K. J.: Clouds and the Faint Young Sun Paradox, *Clim. Past*, 7, 203–220, doi:10.5194/cp-7-203-2011, 2011.

Goldblatt, C., Claire, M. W., Lenton, T. M., Matthews, A. J., Watson, A. J., and Zahnle, K. J.: Nitrogen-enhanced greenhouse warming on early Earth, *Nat. Geosci.*, 2, 891–896, 30 doi:10.1038/NGEO692, 2009.

Gough, D. O.: Solar interior structure and luminosity variations, *Sol. Phys.*, 74, 21–34, 1981.

Hack, J. J., Sensitivity of the simulated climate to a diagnostic formulation for 554 cloud liquid water, *J Climate*, 11 (7), 1497–1515. 1998

Halevy, I., R. T. Pierrehumbert, and D. P. Schrag, Radiative transfer in CO<sub>2</sub>-rich paleo-atmospheres, *J. Geophys. Res.*, 114, D18112, doi: 10.1029/2009JD011915. 2009

Haq-Misra, J. D., Domagal-Goldman, S. D., Kasting, P. J., and Kasting, J. F.: A revised, hazy methane greenhouse for the archaic Earth, *Astrobiology*, 8, 1127–1137, 2008.

Hartmann, D. L., and M. L. Michelsen: No evidence for iris. *Bull. Amer. Meteor. Soc.*, 83, 249–254. 2002

Hartmann, D. L., and M. L. Michelsen, *Bull. Amer. Meteor. Soc.*, 83, 1349–1352. 2002

Hay, W. W., Migdisov, A., Balukhovskiy, A. N., Wold, C. N., Flågel, S., and S. Á

C1516

oding, E.: Evaporites and the salinity of the ocean during the Phanerozoic: implications for climate, ocean circulation and life, *Palaeogeogr. Palaeoclimatol.*, 240, 3–46, doi:10.1016/j.palaeo.2006.03.044, 2006.

Jacob, R.: Low frequency variability in a simulated atmosphere ocean system, PhD Thesis, University of Wisconsin-Madison, 1997–310 pp., 1997.

Jenkins, G. S.: The effects of reduced Eland fraction and solar forcing on the general – circulation – results from the NCAR CCM, *Glob. Planet. Change*, 7, 321–333, 1993.

Jenkins, G.S., Marshall, H.G., Kuhn, W.R., Precambrian climate – the effects of land area and Earth's rotation rate. *JGR-atmosphere*, volume: 98, issue: D5, pages: 8785-8791, DOI: 10.1029/93JD00033, 1993,

Kasting, J. F.: The evolution of the prebiotic atmosphere, *Origins Life Evol. B.*, 14, 75–82, 1984. 10

Kasting, J. F.: Theoretical constraints on oxygen and carbon-dioxide concentrations in the Pre-cambrian atmosphere, *Precambrian Res.*, 34, 205–229, 1987.

Kasting, J. F.: Early Earth faint young sun redux, *Nature*, 464, 687–689, 2010.

Kiehl, J. T. and Dickinson, R. E.: A study of the radiative effects of enhanced atmospheric CO<sub>2</sub> and CH<sub>4</sub> on early Earth surface temperatures, *J. Geophys. Res.-Atmos.*, 92, 2991–2998, 15 1987.

Kienert, H., Feulner, G., and Petoukhov, V.: Faint young sun problem more severe due to ice-albedo feedback and higher rotation rate of the early Earth, *Geophys. Res. Lett.*, 39, L23710, doi:10.1029/2012GL054381, 2012.

Knauth, L. P.: Temperature and salinity history of the Precambrian ocean: implications for the course of microbial evolution, *Palaeogeogr. Palaeoclimatol.*, 219, 53–69, 2005.

Kump, L. R. and Pollard, D.: Amplification of cretaceous warmth by biological cloud feedbacks, *Science*, 320, 195–195, 2008.

C1517

Le Hir, G., Donnadieu, Y., Godd'eres, Y., PierreHumbert, R. T., Halverson, G., Macouin, M., Nedelec, A., and Ramstein, G.: The snowball Earth aftermath: exploring 25 the limits of continental weathering processes, *Earth Planet. Sci. Lett.*, 277, 453–463, doi:10.1016/j.epsl.2008.11.010, 2009.

Le Hir, G., Donnadieu, Y., Krinner, G., and Ramstein, G.: Toward the snowball earth deglaciation, *Clim. Dynam.*, 35, 285–297, 2010.

Le Hir G., Donnadieu Y., Godd'eres Y., Meyer-Berthaud B., Ramstein G., and Blakey, R. C.: The climate change caused by the land plant invasion in the Devonian, *Earth Planet. Sci. Lett.*, 310, 203–212, 2011.

Millero, F. J. and Poisson, A.: International one-atmosphere equation of state of seawater, *Deep-Sea Res. Pt. I*, 28, 625–629, 1981.

Nardin, E., Godd'eres, Y., Donnadieu, Y., Le Hir, G., Blakey, R. C., Puc'eat, E., and Aretz, M.: Modeling the early Paleozoic long-term climatic trend, *Geol. Soc. Am. Bull.*, 123, 1181–1192, 2010. 5

Pesonen, L. J., Elming, S. A., Mertanen, S., Pisarevsky, S., D'Agrella-Filho, M. S., Meert, J. G., Schmidt, P. W., Abrahamsen, N., and Bylund, G.: Palaeomagnetic configuration of continents during the Proterozoic, *Tectonophysics*, 375, 289–324, 2003.

Pierrehumbert, R. T.: High levels of atmospheric carbon dioxide necessary for the termination of global glaciation, *Nature*, 429, 646–649, 2004.

Pierrehumbert R.T.: *Principles of Planetary Climate*. Cambridge University Press, 652pp. 2010

Pierrehumbert, R.T., Abbot D.S., Voigt., A. and Koll D., *Climate of the Neoproterozoic Annual Review of Earth and Planetary Sciences Vol. 39: 417-460*, DOI: 10.1146/annurev-earth-040809-152447. 2011

Poulsen, C. J. and Jacob, R. L.: Factors that inhibit snowball Earth simulation,

C1518

*Paleoceanography*, 19, PA4021, doi:10.1029/2004PA001056, 2004.

Reinhard, C. T. and Planavsky, N. J.: Mineralogical constraints on Precambrian p(CO<sub>2</sub>), *Nature*, 474, E1–E2, doi:10.1038/nature09959, 2011.

Rondanelli, R. and Lindzen, R. S.: Can thin cirrus clouds in the tropics provide a solution to the faint young Sun paradox?, *J. Geophys. Res.-Atmos.*, 115, D02108, doi:10.1029/2009JD012050, 2010.

Rosing, M. T., Bird, D. K., Sleep, N. H., and Bjerrum, C. J.: No climate paradox under the faint early Sun, *Nature*, 464, 744–747, doi:10.1038/nature08955, 2010.

Rossow, W. B., Henderson-Sellers, A., and Weinreich, S. K.: Cloud feedback – a stabilizing effect for the early Earth, *Science*, 217, 1245–1247, 1982.

Rye, R., Kuo, P. H., and Holland, H. D.: Atmospheric carbon-dioxide concentrations before 2.2-billion years ago, *Nature*, 378, 603–605, 1995.

Sagan, C. and Mullen, G.: Earth and Mars – evolution of atmospheres and surface temperatures, *Science*, 177, 52–56, doi:10.1126/science.177.4043.52, 1972. 25

Schatten, K. H. and Endal, A. S.: The faint young Sun climate paradox – volcanic influence, *Geophys. Res. Lett.*, 9, 1309–1311, doi:10.1029/GL009i012p01309, 1982.

Sheldon, N. D.: Precambrian paleosols and atmospheric CO<sub>2</sub> levels, *Precambrian Res.*, 147, 148–155, 2006.

Stevens, B.; Bony, S, *What Are Climate Models Missing?* *Science*, Vol. 340, No. 6136. pp. 1053-1054, doi:10.1126/science.1237554. 2013

Voigt, A. and Abbot, D. S., Sea-ice dynamics strongly promote Snowball Earth initiation and destabilize tropical sea-ice margins, *Clim. Past*, 8, 2079-2092, doi:10.5194/cp-8-2079-2012, 2012,

Walker, J.C.G., Hays, P.B. and Kasting, J.F., *A Negative Feedback Mechanism For*

C1519

The Long-Term Stabilization of Earth's Surface-Temperature. *Journal Of Geophysical Research-Oceans And Atmospheres*, 86(NC10): 9776-9782. 1981

Walker, J. C. G.: Climatic factors on the Archean Earth, *Palaeogr. Palaeocl.*, 40, 1–11, 30 doi:10.1016/0031-0182(82)90082-7, 1982.

Walker, J. C. G. and Zahnle, K. J. Lunar nodal tide and distance to the Moon during the Pre-cambrian, *Nature*, 320, 600–602, 1986.

Williams, P. D., Guilyardi, E., Madec, G., Gualdi, S., and Scoccimarro, E.: The role of mean ocean salinity in climate, *Dyn. Atmos. Oceans*, 49, 108–123, doi:10.1016/j.dynatmoce.2009.02.001, 2010.

Wordsworth, R. and Pierrehumbert. R.: Hydrogen-nitrogen greenhouse warming in Earth's early atmosphere, *Science*, 339, 64–67, doi:10.1126/science.1225759, 2013.

Interactive comment on *Clim. Past Discuss.*, 9, 1509, 2013.

C1520

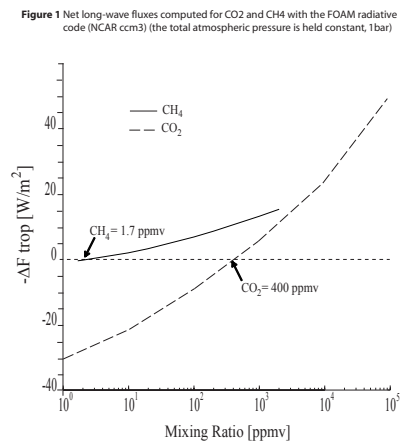
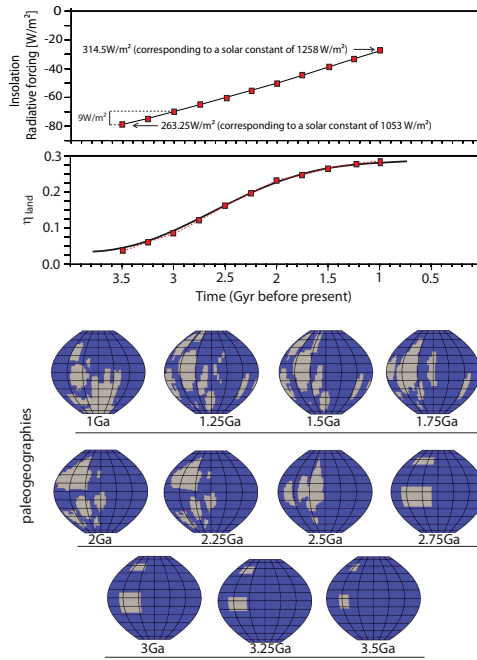


Fig. 1.

C1521

**Figure 2:** boundary conditions for solar constant (upper part) and continental growth (lower part).  $\eta_{land}$  is the emerged surface/Earth surface (present-day surface is  $146.10^6 \text{ km}^2$  or 29% of the Earth surface). Each red square represents boundary conditions used in our sets of simulations.



**Fig. 2.**

C1522

**Figure 3:** 3D climate simulations from 3.5 to 1 Gyr. a) Evolution of surface temperature versus time assuming increasing irradiance, linear continental growth and  $\text{pCO}_2$  and  $\text{pCH}_4$  of 900ppmv. Grey line is from Rosing et al (2010). Blue and red lines were obtained using liquid droplets size of 5 to  $10 \mu\text{m}$  (modern clouds) and  $20 \mu\text{m}$  (optically thinner clouds), respectively. Green squares represent the no-clouds scenario. b) Evolution of planetary albedo versus time (ocean 0.06, rocky desert continents 0.32, ice 0.5, snow 0.8). c) Red stars represent sea-ice extend (white) predicted with runs performed with liquid droplets size of  $20 \mu\text{m}$  (fig3a, and b show corresponding temperature/albedo for each simulation).

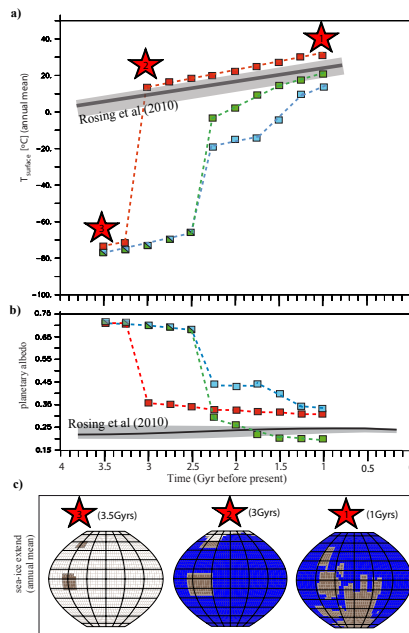


**Fig. 3.**

C1523

**Figure 4:** a) Net cloud radiative forcing (CRF, unit  $W/m^2$ ) versus time. Blue squares represent runs with modern clouds. Optically thinner clouds (red squares) result in a positive forcing because the effect of infra-red trapping overcomes that of scattering.  
 b) CRF as a function of latitude for simulations performed at 1 Ga. The black line represents low CCN clouds (liquid droplets size of  $20\mu m$ ), dashed line the modern clouds parameterization (liquid droplets size of 5 to  $10\mu m$ ). c) Simulations performed using 1Ga boundary conditions. Dashed lines represent long-wave (LW) budget of clouds (greenhouse effect), continuous lines their short wave budget (albedo effect).

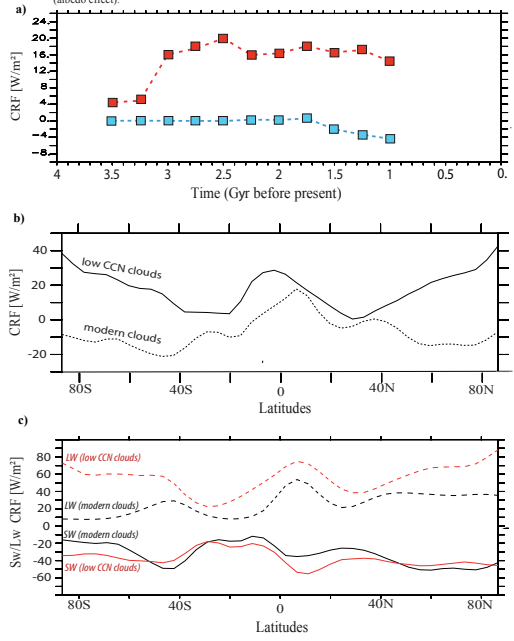


**Fig. 4.**

C1524

**Figure 5:** a) Faster rotation (16 hours of LOD), saltier ocean and pCO<sub>2</sub> impacts on the FISP 3.5Ga ago (table 1b). Red diamonds represent simulations with standard conditions (pCH<sub>4</sub> fixed at 900ppmv, low CCN clouds), yellow diamond (standard cond. + saltier ocean), green diamond (standard cond. + 16h of LOD), blue diamond (standard cond. + saltier ocean + 16h of LOD). At 1800 ppmv of CO<sub>2</sub> the surface temperature reaches respectively 14.2°C, 15.0°C, 14.2°C, 14.4°C. b) The sea surface temperature (SST) response to a faster rotation (LOD) and/or saltier ocean obtained with a fixed pCO<sub>2</sub> at 1.8mbars (1800ppmv or 6.4PAL).

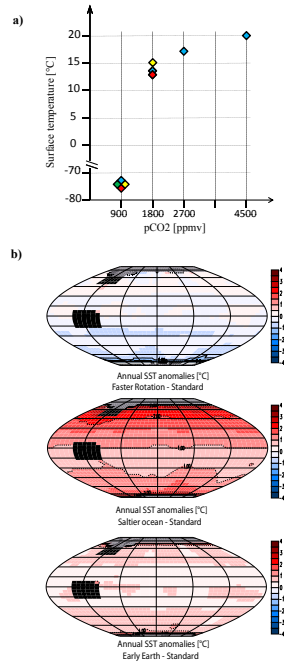


**Fig. 5.**

C1525

**Annexe 1: a)** temperature gradient as a function of Earth rotation rates. **b)** Atmospheric lapse rate of function of ozone layer presence/removing. Simulations performed using present day boundary conditions.

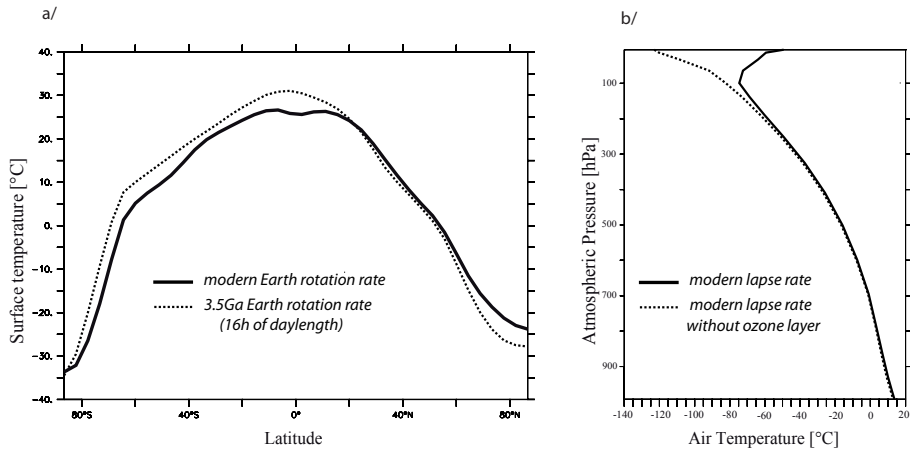


**Fig. 6.**

C1526

Table 1a. Summary of simulations (900ppmv of CO<sub>2</sub> and CH<sub>4</sub>) (sections 3.1 - 3.3)

set of simulations	Boundary conditions		LOD (hours)	Droplet size(µm)	seawater freezing point
	Paleogeography	Solar constant			
modern clouds	3.5-1Ga (fig.2)	3.5-1Ga (fig.2)	24	5-10	-1.8°C
no clouds	"	"	24	/	"
low CCN clouds	"	"	24	20	"

Table 1b. Summary of simulations carried out with CO<sub>2</sub> concentration set to 900, 1800, 2700 and 4500ppmv (900ppmv of pCH<sub>4</sub>) (sections 3.4 and 3.5)

set of simulations	Boundary conditions		LOD (hours)	Droplet size(µm)	seawater freezing point
	Paleogeography	Solar constant			
Standard conditions	3.5Ga	3.5Ga (1033W/m <sup>2</sup> )	24	20	-1.8°C
Saliner ocean	"	"	24	"	-3.3°C
Faster Rotation	"	"	16	"	-1.8°C
Early Earth	"	"	16	"	-3.3°C

**Fig. 7.**

C1527

Table 2. Sensitivity runs showing alternative solutions to the faint young Sun (section 4)

set of simulations	Boundary conditions	pCO <sub>2</sub> (10 <sup>3</sup> bar)	pCH <sub>4</sub> (10 <sup>3</sup> bar)	Ice albedo Vis / nIR	LOD (hours)	Droplet size(μm)	Global Ts (°C)
Run1	3.5Ga	25.2	1.7	0.7/0.5	24	20	18.5
Run2	"	16.8	"	"	"	"	15.7
Run3	"	8.4	"	"	"	"	<0°C*
Run4	"	25.2	"	"	"	5-10	-73
Run5	"	56.0	"	"	"	"	15.5
Run6	"	112.0	"	"	"	"	21.1
Run7	"	28.2	"	0.5/0.5 <sup>†</sup>	"	"	-10.5

\* no stabilized cooling

<sup>†</sup> visible snow albedo fixed to 0.7 (instead of 0.9)

Fig. 8.

C1528